The Plant Cell, Vol. 17, 2204–2216, August 2005, www.plantcell.org 

# Control of Root Cap Formation by MicroRNA-Targeted Auxin Response Factors in Arabidopsis [W]

**Jia-Wei Wang,[a,b] Ling-Jian Wang,[a] Ying-Bo Mao,[a,b] Wen-Juan Cai,[a] Hong-Wei Xue,[a] and Xiao-Ya Chen[a,1]**

[a] National Key Laboratory of Plant Molecular Genetics, Institute of Plant Physiology and Ecology, Shanghai Institutes for Biological Sciences, Chinese Academy of Sciences, Shanghai 200032, People's Republic of China
[b] Graduate School of Chinese Academy of Sciences, Shanghai 200032, People's Republic of China

**The plant root cap mediates the direction of root tip growth and protects internal cells. Root cap cells are continuously produced from distal stem cells, and the phytohormone auxin provides position information for root distal organization. Here, we identify the *Arabidopsis thaliana* auxin response factors ARF10 and ARF16, targeted by microRNA160 (miR160), as the controller of root cap cell formation. The *Pro$_{35S}$:MIR160* plants, in which the expression of *ARF10* and *ARF16* is repressed, and the *arf10-2 arf16-2* double mutants display the same root tip defect, with uncontrolled cell division and blocked cell differentiation in the root distal region and show a tumor-like root apex and loss of gravity-sensing. ARF10 and ARF16 play a role in restricting stem cell niche and promoting columella cell differentiation; although functionally redundant, the two ARFs are indispensable for root cap development, and the auxin signal cannot bypass them to initiate columella cell production. In root, auxin and miR160 regulate the expression of *ARF10* and *ARF16* genes independently, generating a pattern consistent with root cap development. We further demonstrate that miR160-uncoupled production of ARF16 exerts pleiotropic effects on plant phenotypes, and miR160 plays an essential role in regulating Arabidopsis development and growth.**

## INTRODUCTION

The key theme of pattern formation is the precise coordination of cell division and differentiation. In *Arabidopsis thaliana*, the root meristem contains a small number of mitotically inactive central cells, known as the quiescent center (QC), surrounded by four types of stem cells (initials). Each cell type is derived from its own set of initials, and the stem cell division is tightly controlled (Dolan et al., 1993; Scheres et al., 2002). The root cap has a simple structure, which is composed of columella in the central portion and lateral root cap (shedding cells) in the outer portion. The columella initials generally divide only anticlinally, and their daughter cells undergo rapid elongation and differentiation, producing starch granules that mediate gravity sensing (Sack, 1997). The epidermal/shedding cell initials undergo both anticlinal and periclinal divisions (Dolan et al., 1993). The stem cell division and daughter cell differentiation are continuous as the root grows indeterminately, with the outermost cells being detached from the root. The root cap contributes to plant adaptations to environments by its role in sensing gravity and protecting internal root meristem cells.

Auxin is a central hormone in regulating plant life. In roots, the auxin response maximum serves as a positional cue for cell fate determination and distal organization (Sabatini et al., 1999). Mutations in both auxin polar transport facilitators and signaling factors result in defects in root distal cell specification (Sabatini et al., 1999; Friml et al., 2002), yet transcription factors that link the auxin signal to root cap development have not been reported.

The plant response to auxin involves the short-lived auxin/indole-3-acetic acid (Aux/IAA) proteins, the auxin response factors (ARFs), and the components of the protein degradation pathway (Dharmasiri and Estelle, 2004). ARFs bind to auxin response elements in promoters of early auxin response genes (Guilfoyle and Hagen, 2001). These transcription factors harbor two conserved domains, an N-terminal DNA binding domain and a C-terminal dimerization domain that shares sequence similarities to motifs III and IV found in Aux/IAA proteins and mediates protein–protein interaction. In response to auxin, Aux/IAAs are targeted for proteolysis through the ubiquitin-mediated pathway, relieving ARFs, which regulate downstream gene transcription (Gray et al., 2001; Serino and Deng, 2003). The Arabidopsis genome contains 23 *ARF* genes, of which only a few have been characterized. MONOPTEROS (MP/ARF5) mediates apical–basal pattern formation in embryo (Berleth and Jürgens, 1993; Hardtke and Berleth, 1998), ETTIN (ETT/ARF3) is involved in gynoecium morphogenesis (Nemhauser et al., 2000), and NONPHOTOTROPIC HYPOCOTYL 4 (NPH4/ARF7), ARF19, and ARF2 participate in controlling differential cell growth (Stowe-Evans et al., 1998; Harper et al., 2000, Li et al., 2004; Okushima et al., 2005). Furthermore, MP and NPH4 have partial functional redundancy (Hardtke et al., 2004), and both are positive regulators of the *PLETHORA* (*PLT*) genes, which encode AP2-type putative transcription factors and determine the root stem cell niche (Aida et al., 2004).

[1] To whom correspondence should be addressed. E-mail xychen@sibs.ac.cn; fax 0086-21-54924015.
The author responsible for distribution of materials integral to the findings presented in this article in accordance with the policy described in the Instructions for Authors (www.plantcell.org) is: Xiao-Ya Chen (xychen@sibs.ac.cn).
[W] Online version contains Web-only data.
Article, publication date, and citation information can be found at www.plantcell.org/cgi/doi/10.1105/tpc.105.033076.

In addition to phytohormones, microRNAs (miRNAs) also regulate plant development and physiology (reviewed in Bartel, 2004). Analyses of the *hyponastic leaves1* mutant have further suggested the involvement of these small regulatory RNAs in phytohormone responses (Lu and Fedoroff, 2000; Han et al., 2004; Vazquez et al., 2004). At least 22 families of miRNAs in Arabidopsis have been identified to date (Reinhart et al., 2002; Bonnet et al., 2004; Jones-Rhoades and Bartel, 2004; Sunkar and Zhu, 2004; Adai et al., 2005); among them, miRNA160 (miR160) has sequence complementarities to a group of *ARF* genes: *ARF10*, *ARF16*, and *ARF17*. Recent investigations have implicated the importance of miR160 regulation of *ARF17* in maintaining proper auxin homeostasis and the development of plant organs, including adventitious roots (Mallory et al., 2005; Sorin et al., 2005). Here, we show that *ARF10* and *ARF16* control root cap formation. In addition, we demonstrate that the regulation of *ARF16* expression by miR160 is required to maintain the normal growth and development of aerial organs and lateral root production.

## RESULTS

### Cleavage of *ARF* Transcripts by miR160

The Arabidopsis auxin response factors ARF10 (At2g28350), ARF16 (At4g30080), and ARF17 (At1g77850) share high amino acid sequence similarities and form a subgroup in the ARF family (Guilfoyle and Hagen, 2001; Remington et al., 2004; Okushima et al., 2005). They all contain an additional stretch of 32 to 36 amino acids in the DNA binding domain. ARF17 is distinct in that its C-terminal domain is poorly conserved (Okushima et al., 2005). In mRNAs of each of these three genes, there is a fragment that can be recognized by miR160 (Figure 1A). Transcripts of all three genes were detected in roots, stems, leaves, and inflorescences in RNA gel blot analysis, and *ARF16* exhibited a higher level of transcript accumulation than the other two genes (Figure 1B). Besides normal transcripts of the expected size, smaller fragments were detected for all three genes, indicating the presence of cleaved products (Figure 1B). Consistent with the target gene expression, miR160 was found in all of the tissues examined (Figure 1B), suggesting that the three closely related *ARF* genes are also posttranscriptionally regulated.

The miR160-resistant versions of *ARF10*, *ARF16*, and *ARF17* were generated by introducing synonymous substitutions that changed the miR160-paring sequence (Figure 1A). In the Arabidopsis genome, there are three genes that are predicted to encode miR160: *MIR160a*, *MIR160b*, and *MIR160c* (Reinhart et al., 2002). We performed an *Agrobacterium tumefaciens*–mediated transient assay by coexpressing the miR160 genes ($Pro_{35S}$:*MIR160a*, *-b*, or *-c*) with the *ARF* genes ($Pro_{35S}$:*ARF10*, *-16*, or *-17*) or with their mutated versions ($Pro_{35S}$:*mARF10*, *-16*, and *-17*) in tobacco (*Nicotiana benthamiana*) leaves. Three days after inoculation, the wild-type *ARF* mRNAs were efficiently cleaved in the presence of $Pro_{35S}$:*MIR160*, whereas the mutant mRNAs were completely resistant (Figure 1C; data not shown for *ARF10* and *ARF17*). These data confirm the in planta activity of miR160 in cleaving transcripts of the three *ARF* genes.

### Root Cap Defects in $Pro_{35S}$:*MIR160c* and *arf10-2 arf16-2* Plants

The overlapping expression patterns and high sequence similarities imply a functional redundancy shared by ARF10, ARF16, and ARF17. Indeed, plants that carried a T-DNA insertion in either *ARF10* (*arf10-2*) or *ARF16* (*arf16-2*) did not exhibit any visible phenotypic changes according to a vertical plate assay (Figures 2A and 2B) (Okushima et al., 2005). To circumvent the redundancy, we downregulated the gene expression by overexpressing miR160 with the *35S* promoter of *Cauliflower mosaic virus*. In 20-d-old transgenic plants carrying the $Pro_{35S}$:*MIR160a*, *-b*, or *-c* construct, respectively, the full-length transcripts of the three *ARF* genes were barely detectable, whereas the level of cleaved products was increased substantially (Figure 2C).

Because the $Pro_{35S}$:*MIR160a*, *-b*, and *-c* plants displayed the same phenotype, we chose the $Pro_{35S}$:*MIR160c* line for further analysis. Compared with the wild type, the root length of the $Pro_{35S}$:*MIR160c* seedlings was reduced and the lateral root number was increased (Table 1). A more drastic phenotypic change of the $Pro_{35S}$:*MIR160c* plants is that their roots did not grow downward in response to gravity; instead, the root tip growth exhibited frequent changes of direction (Figure 2A). Of the 40 independent $Pro_{35S}$:*MIR160c* lines examined, 36 displayed this phenotypic change, and the severity correlated with the level of transgene expression (data not shown). When 4-d-old vertically grown seedlings were rotated by 90° clockwise, the wild-type root tips turned nearly 90° accordingly, but the $Pro_{35S}$:*MIR160c* root tips did not respond to this orientation change, and their growth directions remained largely unchanged (see Supplemental Figure 1 online). Because plants sense the gravity stimulus by root cap columella cells, which characteristically contain amyloplasts, we examined the root tip organization. The root apex of $Pro_{35S}$:*MIR160c* seedlings swelled with extra cells in the root cap region. Staining the root tip with 1% Lugol solution revealed no starch granules (Figure 2D), corroborating the absence of a gravitropic response.

To determine whether the root cap defect was caused by repressed production of the target ARFs or by other effects of miR160 overproduction, we introduced miR160-resistant *ARFs* driven by their own promoters ($Pro_{ARF10}$:*mARF10*, $Pro_{ARF16}$:*mARF16*, or $Pro_{ARF17}$:*mARF17*) into the $Pro_{35S}$:*MIR160c* plants. In F1 plants expressing either *mARF10* or *mARF16*, root cap development was completely restored, and thus the gravitropism, whereas root caps were not recovered when the wild-type gene was introduced. *mARF17*, however, failed to rescue root cap development (Figure 2A), consistent with the observation that *ARF17* transcripts were undetectable in root tips (Birnbaum et al., 2003) (data not shown).

To further confirm the role of ARF10 and ARF16 in root cap formation, we generated the *arf10-2 arf16-2* double mutant. As expected, homozygous *arf10-2 arf16-2* plants displayed the same phenotype as the $Pro_{35S}$:*MIR160c* plants, with the loss of columella cell identity and excessive cell division in the root distal region and, subsequently, agravitropic root growth (Figures 2A and 2D, Table 1; see Supplemental Figure 1 online). The root cap defect of the double mutant seemed slightly different and less severe: the cells were irregularly expanded, and a small amount

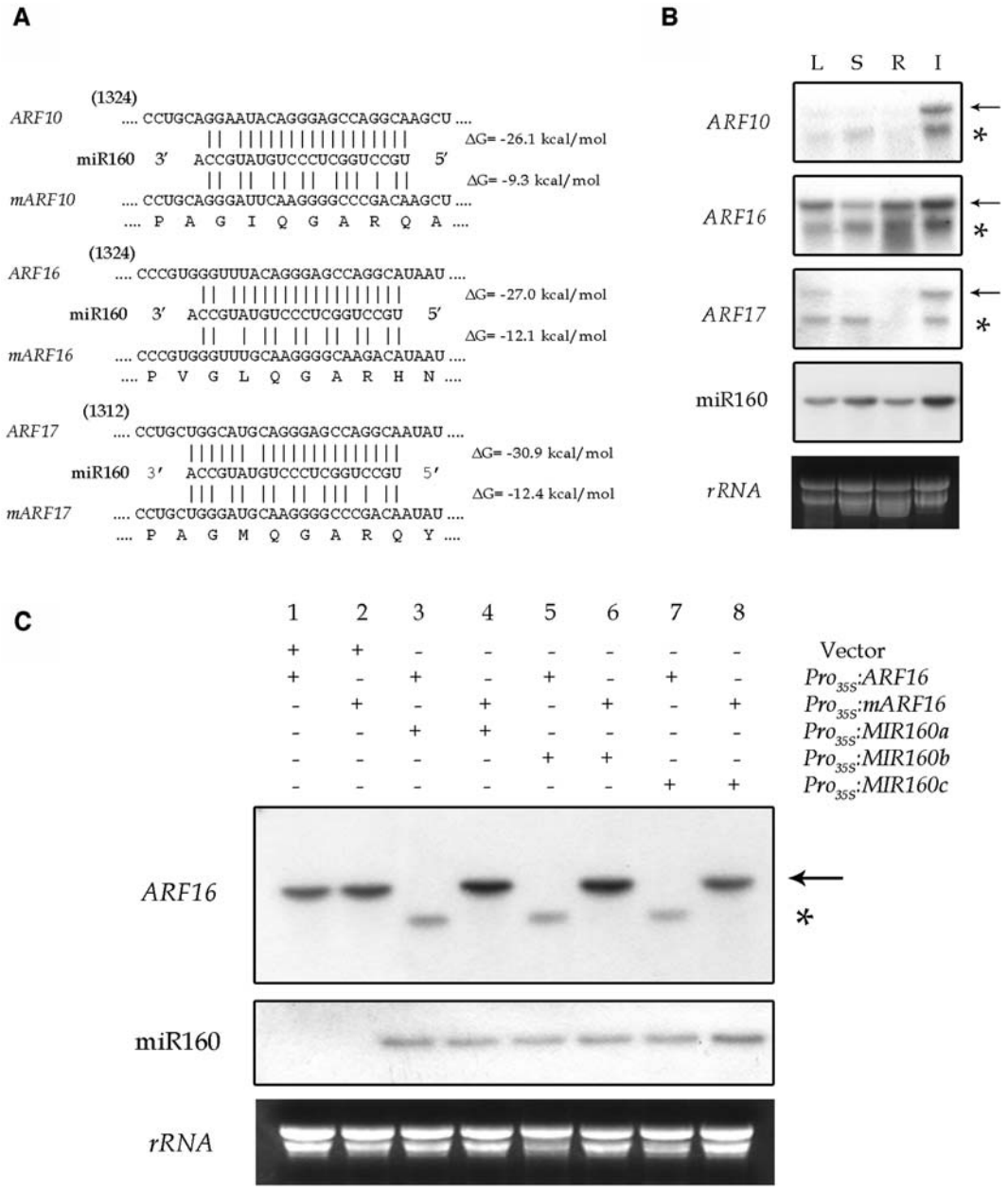


**Figure 1.** Expression of *ARF10*, *ARF16*, and *ARF17* in Plants, and Regulation by miR160.

**(A)** Alignment of partial mRNA sequences of *ARF10*, *ARF16*, *ARF17*, and miR160. Free energies of duplex structures were calculated using the Mfold method (Zuker, 2003). *mARF10*, *mARF16*, and *mARF17* are the modified mRNAs that harbor synonymous nucleotide substitutions in miR160 binding sites.

**(B)** Expression of miR160, *ARF10*, *ARF16*, and *ARF17* in Arabidopsis. Total RNAs from rosette leaf (L), stem (S), root (R), and inflorescence (I) were examined by RNA gel blot analysis with the radiolabeled probes indicated.

**(C)** Cleavage of *ARF16* transcripts by miR160 in planta. Constructs harboring the wild-type or the mutated *ARF16* driven by the *35S* promoter were coagroinoculated with the $Pro_{35S}$:*MIR160* construct in tobacco leaves. The empty vector of pKYLX71 (Vector) was used as a negative control. Total RNAs were extracted after a 3-d inoculation and examined by RNA gel blot analysis.

Arrows and asterisks indicate the full-length and 3′ cleaved products of each mRNA, respectively.

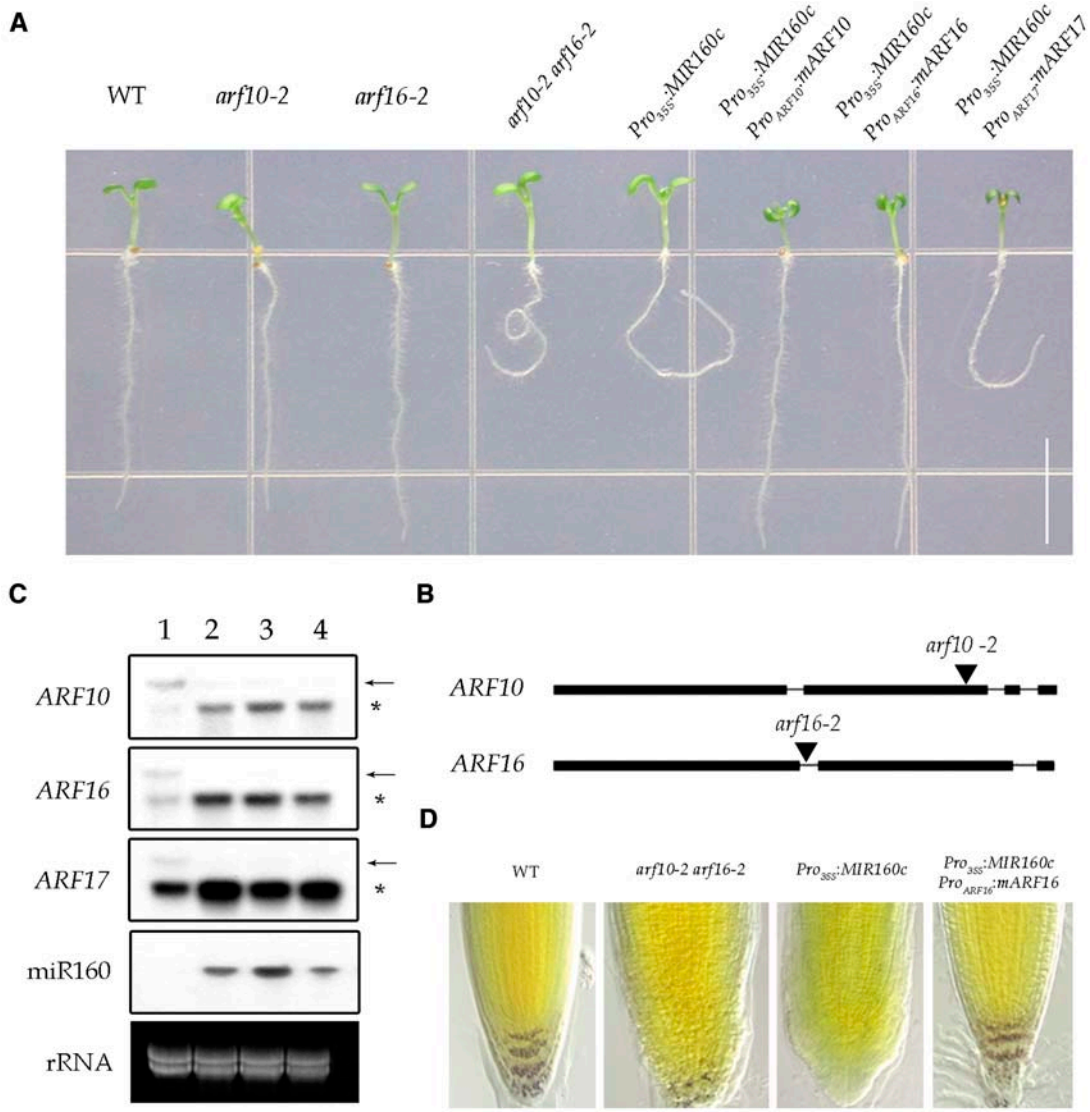


**Figure 2.** ARF10 and ARF16 Control Root Cap Formation.

**(A)** Five-day-old seedlings showing agravitropic root growth (*arf10-2 arf16-2*, *Pro*$_{35S}$*:MIR160c*, and *Pro*$_{35S}$*:MIR160c Pro*$_{ARF17}$*:mARF17*) and rescue by expressing *ARF10* or *ARF16* (*Pro*$_{35S}$*:MIR160c Pro*$_{ARF10}$*:mARF10*, *Pro*$_{35S}$*:MIR160c Pro*$_{ARF16}$*:mARF16*). *Pro*$_{ARF17}$*:mARF17* failed to rescue the gravitropism. WT, wild type. Bar = 0.5 cm.

**(B)** Schemes of T-DNA insertion mutants of *arf10-2* and *arf16-2*. Black boxes and lines represent exons and introns, respectively. Triangles indicate the T-DNA insertion site.

**(C)** RNA gel blot of the *ARF* transcripts in 20-d-old wild-type (lane 1), *Pro*$_{35S}$*:MIR160a* (lane 2), *Pro*$_{35S}$*:MIR160b* (lane 3), and *Pro*$_{35S}$*:MIR160c* (lane 4) plants. In plants ectopically overexpressing miR160, most of the target transcripts were decreased and the level of cleaved products was increased. Arrows and asterisks indicate the full-length and 3′ cleaved products of each mRNA, respectively.

**(D)** Root tip and starch granules (stained purple) of 5-d-old seedlings.

of starch granules was observed (Figures 2D and 3A). It is possible that the T-DNA insertion in *arf10-2* (near the 3′ end) did not result in a complete loss of its function. RT-PCR revealed that the 5′ truncated mRNA was indeed detectable (data not shown).

Together, the data gathered from the T-DNA insertion mutants and miR160-overexpressing lines demonstrate that ARF10 and ARF16 are required for root cap development, whereas ARF17 is not involved in this process.

### Cell Division and Cell Patterning of *Pro*$_{35S}$*:MIR160c* and *arf10-2 arf16-2* Roots

In wild-type Arabidopsis, the columella root cap harbors three tiers of cells, t1 to t3 (Dolan et al., 1993). After anticlinal division from columella initials, the number of columella cells per tier is maintained and periclinal division is rare (Figure 3A). Both *Pro*$_{35S}$*:MIR160c* and *arf10-2 arf16-2* roots, however, had additional and

**Table 1.** Quantitative Effects of ARF10, ARF16, and miR160 on Root Growth

| Seedling Type | Primary Root Length (mm) | Lateral Root Number |
|---|---|---|
| Wild type (Col-0) | 39.86 ± 3.50 | 5.33 ± 1.01 |
| *Pro$_{35S}$:MIR160c* | 23.18 ± 5.44[a] | 8.70 ± 1.15[a] |
| *arf10-2* | 39.45 ± 2.70 | 5.10 ± 0.98 |
| *arf16-2* | 40.11 ± 2.52 | 5.25 ± 0.97 |
| *arf10-2 arf16-2* | 32.15 ± 4.90[a] | 7.20 ± 1.30[a] |
| *Pro$_{ARF16}$:ARF16* | 40.15 ± 4.25 | 5.38 ± 1.23 |
| *Pro$_{ARF16}$:mARF16* | 42.55 ± 4.50[b] | 3.00 ± 1.26[a] |

The seedlings were grown vertically for 9 d under continuous light. For each line, ~30 seedlings were scored.
[a] Significantly different compared with the wild type ($P < 0.001$) by Student's *t* test.
[b] Significantly different compared with the wild type ($0.01 < P < 0.02$) by Student's *t* test.

randomly orientated cell divisions in the distal region, leading to supernumerary cells (Figure 3A). In wild-type roots, the columella cells were elongated rapidly. By contrast, such elongation did not occur in either *Pro$_{35S}$:MIR160c* or *arf10-2 arf16-2* roots, in which the distal cells were irregular in shape and the cell stratification was gradually disturbed (Figure 3A). In addition, the root apex malformation of the *Pro$_{35S}$:MIR160c* and *arf10-2 arf16-2* seedlings was progressively more severe as the uncontrolled cell proliferation continued, and the outermost cells were not detached.

To further visualize cell division, we crossed *Pro$_{35S}$:MIR160c* to a mitotic marker line, *Pro$_{cyc1At}$*:cyclin destruction box (*CDB*)-*GUS* (for β-glucuronidase) (Donnelly et al., 1999). In 6-d-old wild-type roots, cell division was active in the region ~600 μm above the QC, whereas in *Pro$_{35S}$:MIR160c* roots, the GUS activities were extended down to the distal region (Figure 3B), reflecting an ectopic cell division. This observation indicates that in plants expressing *Pro$_{35S}$:MIR160c*, cells in the columella root cap region remain active in cell division.

Next, we introduced several green fluorescent protein (GFP)- and GUS-based cell-specific markers into the *Pro$_{35S}$:MIR160c* plants by crossing to examine root tip cell patterning (Sabatini et al., 1999). The expression domain of the columella initial marker (J2341) was enlarged and occupied several layers of cells, compared with a single layer in wild-type roots (Figure 3C). This, together with the fact that the amyloplast-containing columella cells are absent from the *Pro$_{35S}$:MIR160c* root (Figure 2C), indicates that the daughter cells of columella initials fail to undergo differentiation when the expression of *ARF10* and *ARF16* is blocked. The QC domain, represented by QC25, was also expanded in the *Pro$_{35S}$:MIR160c* root tip, with an extra expression domain in the distal region (Figure 3C). We further investigated the expression of two other markers that are expressed not only in the QC but also in endodermis/cortex (J0571) or the vascular bundle (J2501). We found that, although the organization of the vascular tissue and endodermis/cortex in the *Pro$_{35S}$:MIR160c* root was largely normal, enlargement of the QC expression domain, which overlapped the columella initials marker (J2341), was evident (Figure 3C). These data suggest a mixed identity of the abnormal cells in the *Pro$_{35S}$:MIR160c* root cap region.

### Regulation of *ARF16* Expression by miR160

To reveal the tissue specificity of *ARF16* expression, we generated plants expressing *GUS*- or *GFP-ARF16* chimerical genes: *Pro$_{ARF16}$:GUS-ARF16* and *Pro$_{ARF16}$:GFP-ARF16*. Both fusion proteins were functional in that they rescued the root tip defects of the *arf10-2 arf16-2* mutant plants. In primary roots of transgenic plants carrying *Pro$_{ARF16}$:GFP-ARF16*, the chimerical gene was expressed in columella and lateral root cap cells as well as in progenitor stem cells, and the GFP signal was localized exclusively in the nucleus (Figures 4A and 4B). In emerging lateral

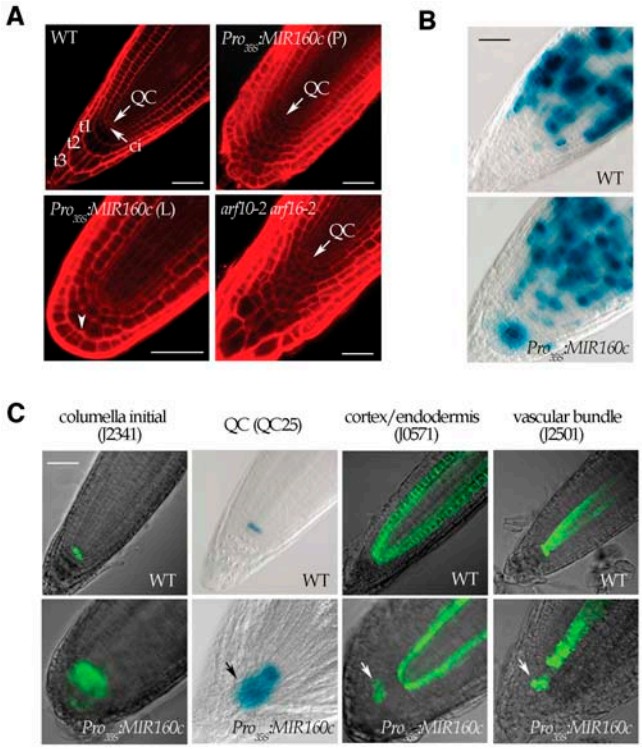


**Figure 3.** Disruption of *ARF10* and *ARF16* Results in Defects in Differentiation and Patterning of Root Distal Cells.

**(A)** Compared with the wild type, the 5-d-old *Pro$_{35S}$:MIR160c* and *arf10-2 arf16-2* seedlings displayed uncontrolled division of undifferentiated cells in the distal regions of both primary (P) and lateral (L) roots. In *Pro$_{35S}$:MIR160c* (L), the arrowhead indicates aberrantly dividing cells. Cell outlines were stained by propidium iodide (red). ci, columella initial; QC, quiescent center; t1 to t3, three columella cell tiers in wild-type root cap. Bars = 50 μm in all panels.
**(B)** Expression of the mitotic marker *Pro$_{cyc1At}$:CDB-GUS* in wild-type (top) and *Pro$_{35S}$:MIR160c* (bottom) roots. In *Pro$_{35S}$:MIR160c*, GUS activity was extended down to the root distal region.
**(C)** Expression of GFP- and GUS-based markers in wild-type (top row) and *Pro$_{35S}$:MIR160c* (bottom row) root tips. Shown are marker lines J2341 for columella initials, QC25 for QC, J0517 for cortex/endodermis, and J2501 for the vascular bundle. Arrows indicates the enlarged expression domain of the QC marker in *Pro$_{35S}$:MIR160c* root.

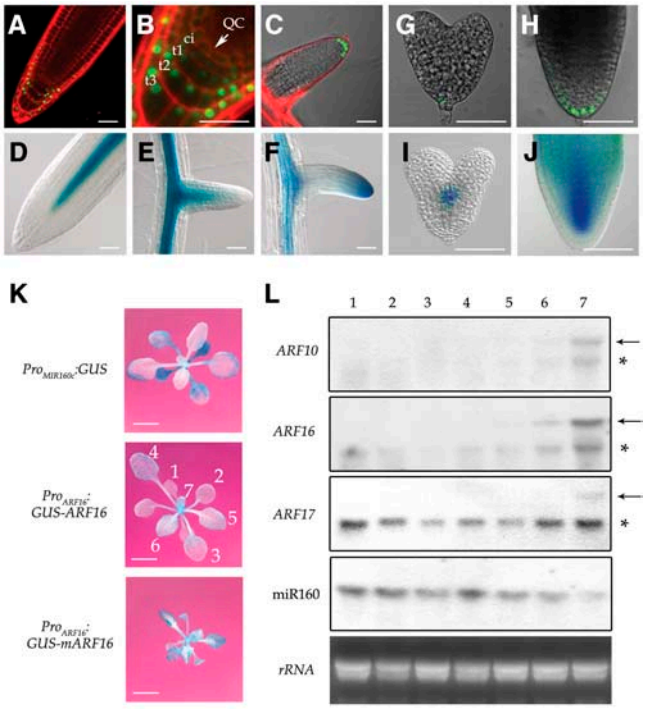


**Figure 4.** Regulation of *ARF16* by miR160.

**(A)** and **(B)** *Pro*$_{ARF16}$*:GFP-ARF16* root, showing *ARF16* expression in distal stem cells and root cap cells and the localization of the GFP-ARF16 fusion protein (green) in the nucleus.

**(C)** The GFP signal provided by *Pro*$_{ARF16}$*:GFP-ARF16* was also present in distal cells of the emerging lateral root.

**(D)** and **(E)** *Pro*$_{MIR160c}$*:GUS* root, showing miR160 expression in the vascular bundle of primary **(D)** and emerging lateral **(E)** roots.

**(F)** *Pro*$_{ARF16}$*:GUS-mARF16* root, showing miR160-uncoupled *ARF16* (*mARF16*) expression in both the root cap region and the vascular bundle.

**(G)** and **(H)** In developing embryos, *ARF16* (*Pro*$_{ARF16}$*:GFP-ARF16*) was expressed in the basal-most region (root cap region) at the heart **(G)** and bent cotyledon **(H)** stages.

**(I)** and **(J)** miR160 (*Pro*$_{MIR160c}$*:GUS*) was detected in the heart-stage embryo **(I)**, and this miRNA then spread throughout the embryo except for the embryonic root cap region **(J)**.

Bars = 50 μm in **(A)** to **(J)**.

**(K)** Expression of *Pro*$_{MIR160c}$*:GUS*, *GUS-ARF16*, and *GUS-mARF16* in leaves of 20-d-old plants. Numbers in the middle panel refer to the order of leaves produced from the plant. Bars = 1.0 cm.

**(L)** RNA gel blot analysis of *ARFs* and miR160 expression in leaves. Lanes 1 to 7 correspond to the order of developing leaves as shown in **(K)**. Full-length transcripts of the *ARF* genes were detected only in younger leaves, whereas miR160 was highly accumulated in older leaves. Arrows and asterisks indicate the full-length and 3′ cleaved products of each mRNA.

roots, the GFP signal was also restricted to the root cap region (Figure 4C). This pattern of expression and subcellular localization of ARF16 is consistent with its role in regulating root cap development as a transcription factor. On the contrary, miR160, as visualized by *Pro*$_{MIR160c}$*:GUS*, was expressed in the vascular bundles of both primary and emerging lateral roots, and GUS activity was never detected in the root apical region (Figures 4D and 4E). Thus, in roots, the spatial distributions of ARF16 and miR160c are nearly complementary to each other.

To assess whether the *ARF16* spatial expression in roots is related to miR160 regulation, we used the *ARF16* promoter to drive *GUS-ARF16* and *GUS-mARF16*. Consistent with *Pro*$_{ARF16}$*:GFP-ARF16*, *Pro*$_{ARF16}$*:GUS-ARF16* was expressed in the root apex (Figure 5A); the *Pro*$_{ARF16}$*:GUS-mARF16* gene, however, was also expressed in the vascular bundle (Figure 4F), indicating that the *ARF16* promoter is active in both the root cap and the vascular bundle. These data suggest a suppression of *ARF16* expression by miR160 in the vascular tissue but not in the root distal region. Therefore, in roots, miR160 helps to restrict the expression of its target *ARF* genes in distal cells.

The expression pattern was then traced back to the embryo. The QC and columella root cap are derived from a single cell, the hypophysis (Scheres et al., 2002). The GFP signal of *Pro*$_{ARF16}$*:GFP-ARF16* began to appear in hypophyseal cells of the heart-stage embryo and then remained in the basal-most region of the embryo (Figures 4G and 4H). The expression of *Pro*$_{MIR160c}$*:GUS* became detectable, also at the heart stage, in the central region, and GUS activity was then spreading in the embryo, except for the embryonic root distal region, with the strongest staining in the provascular bundle (Figures 4I and 4J). Clearly, the spatial expression patterns of *ARF16* and miR160c in the Arabidopsis embryo do not overlap, in accordance with the function of ARF in root distal cells.

We next examined the expression patterns in leaves and found that neither miR160 nor *ARF16* exhibited tissue specificity. The miR160 expression, monitored by GUS staining of the *Pro*$_{MIR160c}$*:GUS* plants, was low or undetectable in juvenile leaves and became high in older leaves. Conversely, *ARF16* expression was high in juvenile leaves, diminished during leaf growth, and was nearly absent in mature leaves (Figure 4K). This downregulation of *ARF16* in developing leaves is clearly mediated by miR160, as *mARF16* expression remained high in old leaves, particularly in the leaf margin (Figure 4K). To detect the transcripts directly, we performed RNA gel blot analysis of *ARF10*, *ARF16*, *ARF17*, and miR160 expression in the first seven leaves of wild-type plants. We found a higher level of expression not only of *ARF16* but also of *ARF10* and *ARF17* in the youngest leaf (Figure 4L, lane 7). By contrast, miR160 production increased gradually during the course of leaf development (Figure 4L). These data suggest a developmentally based regulation of miR160 production, which in turn controls the level of its target *ARF* gene transcripts.

### Auxin Affects *ARF16* Expression in Root

ARFs are downstream components of the auxin signaling pathway. Thus, it is interesting to investigate whether auxin influences *ARF16* expression. RNA gel blot analysis showed that the level of *ARF16* transcripts was increased by approximately threefold after treating the seedlings with 50 μM IAA for 5 h, whereas other phytohormones did not affect *ARF16* expression (see Supplemental Figures 2A and 2B online). The spatial pattern of expression was then examined in *Pro*$_{ARF16}$*:GUS-ARF16* seedlings treated with IAA, which after 12 h induced the expression of this chimerical gene in ectopic positions (Figures 5A and 5B).

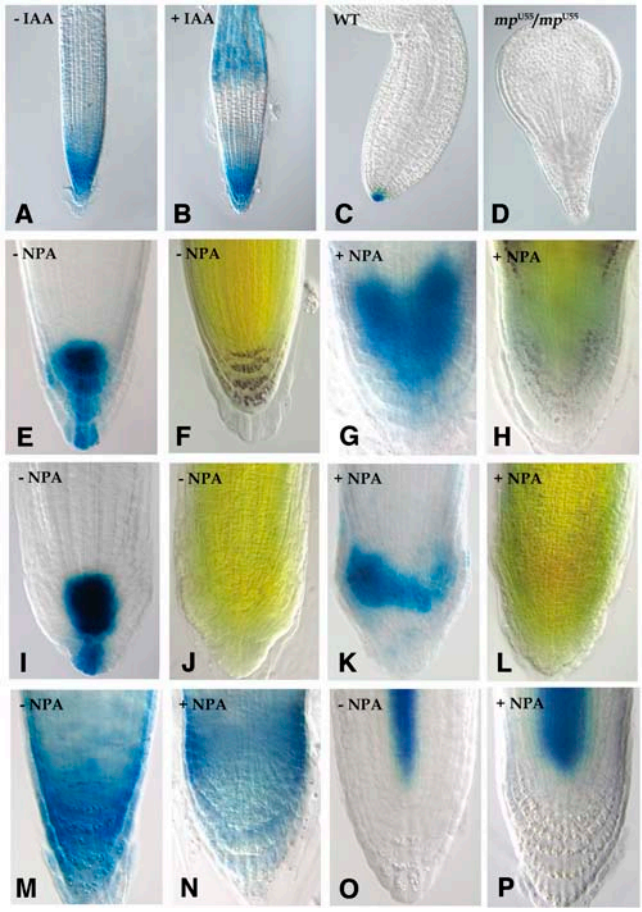


**Figure 5.** Relation between Auxin and *ARF16* Expression in the Root Tip.

**(A)** and **(B)** Ectopic *ARF16* expression induced by auxin in $Pro_{ARF16}$:*GUS-ARF16* roots. The seedlings were treated with **(B)** or without **(A)** 10 μM IAA for 12 h in liquid half-strength MS medium.

**(C)** and **(D)** Accumulation of the GUS-ARF16 fusion protein in wild-type **(C)** and $mp^{U55}/mp^{U55}$ **(D)** embryos. No GUS activity was detected in the heart-stage $mp^{U55}/mp^{U55}$ embryo.

**(E)** to **(H)** Auxin maximum (*DR5-GUS* expression) and starch granules (Lugol staining) in the wild-type root tip, showing the normal auxin maximum in untreated root tips **(E)**, the cup-shaped auxin maximum in NPA-treated root tips **(G)**, and the amyloplast-containing columella cells in untreated **(F)** and NPA-treated **(H)** root tips.

**(I)** to **(L)** $Pro_{35S}$:*MIR160c* root, showing the auxin maximum in untreated **(I)** and NPA-treated **(K)** root tips and the absence of starch granules in untreated **(J)** and NPA-treated **(L)** root tips.

**(M)** and **(N)** Expression of $Pro_{ARF16}$:*GUS-ARF16* in untreated **(M)** and NPA-untreated **(N)** wild-type root tips, showing its association with the auxin maximum.

**(O)** and **(P)** Expression of $Pro_{MIR160c}$:*GUS* in vascular bundles of both untreated **(O)** and NPA-treated **(P)** roots.

Roots in **(E)** to **(P)** were observed 7 d after NPA treatment.

Time-course analysis further demonstrated a slow induction of *ARF16* expression by exogenous auxin, and the transcript level was increased substantially at 5 h after treatment (see Supplemental Figure 2C online), consistent with a previous report (Goda et al., 2004). This delayed response suggests the possible involvement of intermediate factors that link auxin signals to the transcriptional activation of *ARF16*.

*MP* (*ARF5*) has been shown to mediate root meristem formation (Berleth and Jürgens, 1993). The expression of *PLT*, a root stem cell niche marker, is disrupted in the *mp* mutant (Aida et al., 2004). When $Pro_{ARF16}$:*GUS-ARF16* was introduced into $mp^{U55}$ plants, the fusion protein was undetectable in the basal end of $mp^{U55}/mp^{U55}$ embryos (100%; $n = 30$) (Figures 5C and 5D). We also analyzed the fusion gene expression in other auxin transport or signaling mutants, including *pin1*, *axr1-3*, and *tir1-1*. However, no changes in either expression level or position were observed; this is not unexpected because in all of these mutants, columella cell formation appears largely normal (data not shown).

The auxin response maximum functions as a root distal organizer (Sabatini et al., 1999). The involvement of ARF10 and ARF16 in root cap development prompted us to analyze the relation between *ARF* expression and the auxin maximum distribution. In normal growth conditions, the auxin response, as shown by the *DR5-GUS* reporter (Ulmasov et al., 1997), peaked in the region just below the QC (i.e., the columella initials and the columella root cap cells) (Figures 5E and 5F). Treatment of the wild-type root with naphthylphthalamic acid (NPA), an auxin polar transport inhibitor, disturbed auxin flux and resulted in a cup-shaped auxin maximum, together with respecification of the distal cells. The columella root cap cells were enlarged, and the amyloplast-containing cells were present surrounding the abnormal auxin maximum (Figures 5G and 5H) (Sabatini et al., 1999). In $Pro_{35S}$:*MIR160c* root, the auxin maximum was normally positioned, although moved down slightly because the distal cells were not elongated (Figures 5I and 5J). When NPA was applied, a less typical cup-shaped auxin maximum appeared, but the amyloplast-containing columella cells were not found (Figures 5K and 5L), suggesting that the auxin maximum cannot bypass ARF10 and ARF16 to specify columella cells. Further observation revealed that in wild-type roots, the *ARF16* expression domain overlaying the ectopic columella cells was also reshaped, along with the cup-shaped auxin response maximum, after NPA treatment (Figures 5H, 5M, and 5N). Therefore, *ARF16* expression and columella production are associated with the auxin maximum in both normal and NPA-treated roots. $Pro_{MIR160c}$:*GUS* expression, however, was still in the vascular bundle after NPA treatment (Figures 5O and 5P), implying that miR160c expression is independent of auxin signals.

### Pleiotropic Effects of miR160-Uncoupled *ARF16* Expression

Besides the failure in root cap formation, the miR160-overexpressing plants did not exhibit dramatic changes of development and growth (data not shown). To further assess the biological significance of miR160 regulation, we analyzed the phenotypic changes resulting from $Pro_{ARF16}$:*mARF16* or $Pro_{35S}$:*mARF16* expression, each of which was unpaired from miR160. The $Pro_{ARF16}$:*mARF16* seedlings had fewer lateral roots than wild-type seedlings (Figure 6A, Table 1). This, together with the observation that $Pro_{35S}$:*MIR160c* roots were more branched (Table 1), demonstrates a role of miR160 in promoting lateral root production. The $Pro_{35S}$:*ARF16* root was indistinguishable from the wild-type root, whereas the $Pro_{35S}$:*mARF16* root had fewer

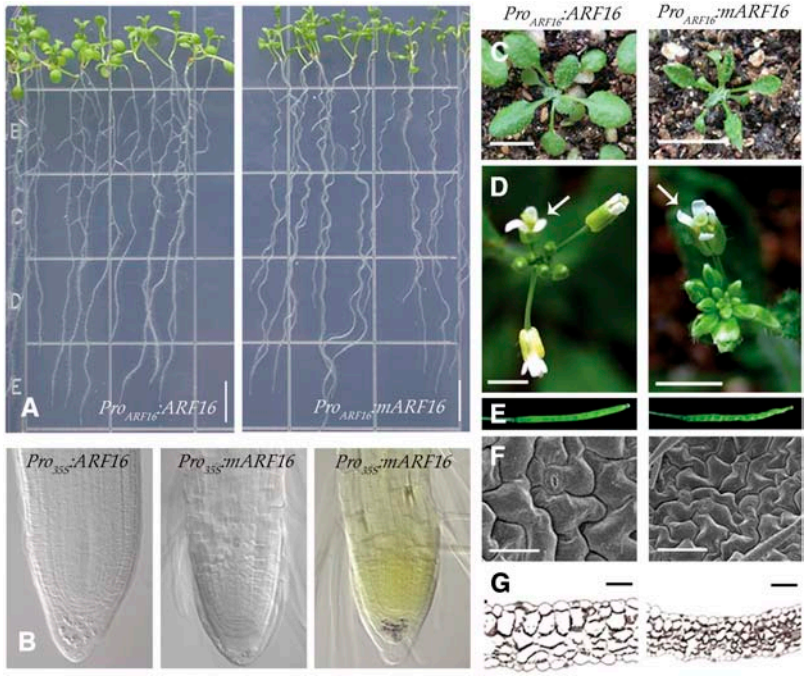


**Figure 6.** The miR160-Uncoupled Expression of *mARF16* Confers Pleiotropic Effects.

**(A)** Root morphology of 7-d-old *Pro*$_{ARF16}$*:ARF16* (left) and *Pro*$_{ARF16}$*:mARF16* (right) seedlings. The *Pro*$_{ARF16}$*:mARF16* seedlings produced fewer lateral roots. Bars = 0.5 cm.

**(B)** Effects of ectopic overexpression of *ARF16* on the root tip. Left, *Pro*$_{35S}$*:ARF16*, which appeared normal; middle, *Pro*$_{35S}$*:mARF16*, showing the consumed basal portion of the root meristem; right, starch granules in the *Pro*$_{35S}$*:mARF16* root tip, which appeared normal.

**(C)** Twenty-day-old *Pro*$_{ARF16}$*:ARF16* (left) and *Pro*$_{ARF16}$*:mARF16* (right) plants. Bars = 1.0 cm.

**(D)** Inflorescences of *Pro*$_{ARF16}$*:ARF16* (left) and *Pro*$_{ARF16}$*:mARF16* (right) plants. Arrows indicate the outward-curled (*Pro*$_{ARF16}$*:ARF16*) and inward-curled (*Pro*$_{ARF16}$*:mARF16*) petals. Bars = 1.0 cm.

**(E)** Siliques of *Pro*$_{ARF16}$*:ARF16* (left) and *Pro*$_{ARF16}$*:mARF16* (right) plants.

**(F)** Scanning electron microscopy views of adaxial epidermal cells of the first rosette leaves of 20-d-old *Pro*$_{ARF16}$*:ARF16* (left) and *Pro*$_{ARF16}$*:mARF16* (right) plants. Bars = 50 μm.

**(G)** Transverse sections of the first rosette leaves of *Pro*$_{ARF16}$*:ARF16* (left) and *Pro*$_{ARF16}$*:mARF16* (right) plants. The *Pro*$_{ARF16}$*:mARF16* leaf had smaller cells, and the cell number per leaf was also reduced (data not shown). Bars = 50 μm.

meristem cells, and the basal cells differentiated immediately above the consumed meristems (Figure 6B). It is possible that ARF16 suppressed cell division in the root meristem; alternatively, ectopic expression of *ARF16* in root meristem cells could disturb the function of other ARFs. Furthermore, the columella cells were normally positioned in *Pro*$_{35S}$*:mARF16* root, with neither ectopic amyloplast-containing cells nor their initials (stem cells) being observed (Figure 6B). This finding suggests that ectopic expression of *ARF16* alone is not sufficient to initiate columella cell formation.

Most of the *Pro*$_{35S}$*:mARF16* seedlings died soon after transferring to pots (data not shown). The surviving plants showed a phenotype resembling that of *Pro*$_{ARF16}$*:mARF16*, and the effect was pleiotropic: plants of both lines were small with miniaturized organs, leaves were upcurled and occasionally serrated, and flowers were aberrant with reduced fertility (Figures 6C to 6E). Observation of the leaf by scanning electron microscopy and transverse cross section revealed a reduction in both cell number and cell size as a result of *Pro*$_{ARF16}$*:mARF16* expression (Figures 6F and 6G; data not shown), indicating a negative effect of the increased level of ARF16 on cell division and cell expansion.

### Increased Expression of Auxin Response Genes in *Pro*$_{ARF16}$*:mARF16* Plants

To analyze the role of miR160 in modulating auxin reactions, we examined *DR5-GUS* expression in *Pro*$_{ARF16}$*:ARF16* and *Pro*$_{ARF16}$*:mARF16* plants. We found that *DR5* activity was greatly enhanced in cotyledons and leaves (mainly the leaf margin) of the *Pro*$_{ARF16}$*:mARF16* plants. In root tips, however, GUS staining remained in the distal region (Figure 7A). The expression of several early auxin response genes, including *IAA1*, *IAA5*, *SAUR-AC1*, *At3g03830*, and *At1g29440*, was then analyzed. We found that the basal expression of all of these genes was higher in *Pro*$_{ARF16}$*:mARF16* than in wild-type and *Pro*$_{35S}$*:MIR160c* plants (Figure 7B). When the seedlings were treated with 50 μM IAA, the expression of these genes was induced dramatically in all three lines. Therefore, overexpression of miR160 does not impair the expression of the tested auxin-induced genes. Together, these data illustrate a role

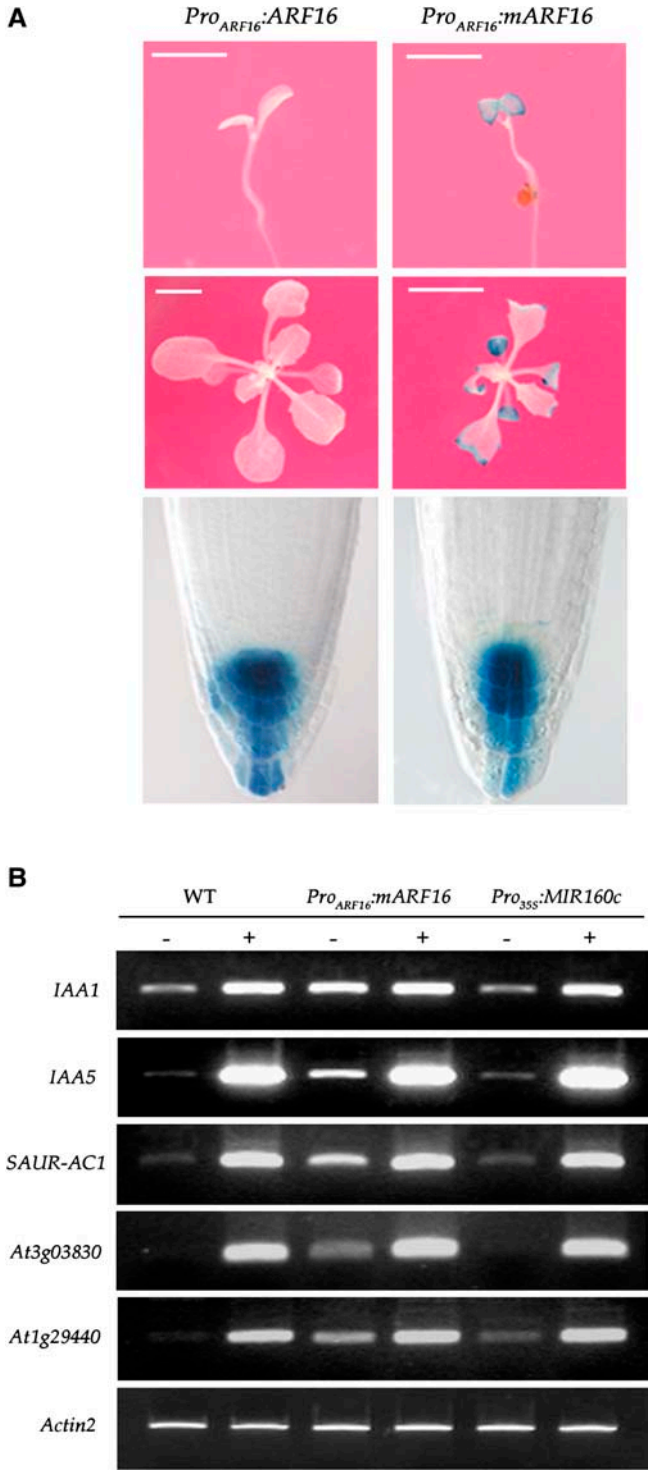


**Figure 7.** *mARF16* Enhances Auxin Response Gene Expression in Plants.

**(A)** *DR5-GUS* expression in $Pro_{ARF16}$:*ARF16* and $Pro_{ARF16}$:*mARF16* plants. The ectopic expression of *DR5* was most evident in the cotyledons and leaf margins when miR160 regulation was impaired. Bars = 0.5 cm.

for the miRNA160-mediated repression of ARF16 in the regulation of basal expression levels, but not of auxin inducibility, in several auxin response genes.

## DISCUSSION

We have identified two auxin response factors, ARF10 and ARF16, as the key controllers of root cap cell differentiation. Data from analysis of the single and double mutants and the miR160-overexpressing lines demonstrate that the two ARFs function redundantly, but as a whole they are indispensable for root cap development.

The root cap cells (i.e., the columella and the lateral root cap cells) are derived from the distal stem cells; thus, a prerequisite for root cap formation is the presence of the stem cells. Two parallel pathways that control QC identity and stem cell niche have been characterized. SHORT-ROOT and SCARECROW, two GRAS family putative transcription factors, play a role in both radial patterning and QC identity, and SCARECROW is required cell autonomously for QC specification (Di Laurenzio et al., 1996; Helariutta et al., 2000; Sabatini et al., 2003). The PLT1 and PLT2 factors provide positional information of the stem cell niche, and auxin directs their spatial expression via ARF5 (MP) and ARF7 (NPH4) (Aida et al., 2004). In addition, PIN and PLT generate an interaction network between auxin transport and root tip cell differentiation (Blilou et al., 2005). However, transcription factors that control the differentiation of specific cell types, such as the columella root cap, have not been identified previously. We provide evidence that ARF10 and ARF16 control root cap formation by restricting cell division and promoting cell differentiation in the distal region. Unlike PLT, which is able to induce ectopic root meristem cells, ARF16 cannot initiate columella production in ectopic positions (Figure 6B). *ARF16* expression in roots is associated with the auxin maximum, and the cup-shaped auxin maximum induced by NPA treatment is accompanied by a similar shape of the *ARF16* expression domain (Figures 5M and 5N). Furthermore, *ARF16* expression was undetectable in the $mp^{U55}/mp^{U55}$ mutant (Figures 5C and 5D). These data place ARF16 (and likely ARF10 as well) downstream of MP and PLT in the auxin-mediated root cap pathway.

In Arabidopsis, both shoot and root meristems show coordinated cell division and differentiation. The *CLAVATA* genes (*CLV1*, *CLV2*, and *CLV3*) encode components of a signaling pathway that promotes the progression of shoot meristem cells, and *clv* mutants develop an enlarged meristem with delayed organ initiation (Schoof et al., 2000; Lenhard and Laux, 2003). The *HOBBIT* (*HBT*) gene encodes a homolog of yeast CDC27/Nuc2, a component of the anaphase-promoting complex; *hbt* mutations reduce root meristem cell division and interfere with the QC and root cap cell specification (Willemsen et al., 1998; Blilou et al., 2002). The role of ARF10 and ARF16 in controlling

**(B)** RT-PCR analysis of auxin response gene expression. The 7-d-old seedlings were treated with 50 μM IAA for 4 h in liquid half-strength MS medium. PCR was performed in 24 cycles for *Actin2* (*At3g18820*) and 30 cycles for early auxin response genes. −, mock treatment; +, auxin treatment.

root cap development elucidated here provides another demonstration that the two processes are inseparable: cell overproliferation in the root distal region is accompanied by impaired cell differentiation and root cap formation.

In addition to the failure of root cap formation, the *Pro$_{35S}$:MIR160c* root also exhibited an enlarged and slightly disturbed stem cell niche (QC and columella initials; Figure 3C). This finding suggests a possible role of ARF10 and ARF16 in repressing *PLT* or other factors that participate in maintaining stem cells surrounding the QC. In shoot, the interaction between *CLV* and *WUSCHEL* genes is required to maintain the stem cell population (Brand et al., 2000; Schoof et al., 2000). Further investigation will reveal whether a similar regulatory loop exists in root.

The *ARF16* gene is expressed not only in columella cells but also in their initials (distal stem cells), despite its role in restraining cell division (Figures 4A and 4B). A positional cue may exist that represses the ARF activity in distal stem cells. The involvement of intracellular signals in stem cell maintenance is a common feature of both plants and animals (Weigel and Jürgens, 2002; Lenhard and Laux, 2003). It is proposed that the QC releases yet unidentified short-range signals that maintain the surrounding stem cells and prevent cell differentiation (van den Berg et al., 1997). The ARF10 and ARF16 identified here may serve as targets of the signal. It will be interesting to determine whether a short-lived QC signal downregulates the activity of ARF10 and ARF16 in the adjacent distal stem cells. The Arabidopsis semidominant *axr3-1* mutant carrying a single nucleotide substitution in an *AUX/IAA* gene (*IAA17*) has a short and agravitropic root without normal columella cell differentiation and *DR5* reporter expression (Leyser et al., 1996; Rouse et al., 1998; Sabatini et al., 1999). The *axr3-1* mutation caused an increased accumulation of AXR3-1/IAA17, and this protein could interact with ARF (Ouellet et al., 2001). Therefore, the defective root cap development in *axr3-1* plants could be related to the suppressed activity of ARF10 and ARF16 at the protein level. This possible protein–protein interaction awaits further investigation.

Plant miRNAs are proposed to direct the clearance of inherited transcription factor mRNAs from specific daughter cell lineages, thereby enabling cell differentiation (Rhoades et al., 2002). Interestingly, in the root distal region, it is the absence of miR160 that ensures root cap cell differentiation. On the other hand, clearance of *ARF* transcripts from the root vascular bundle by miR160 is required to promote lateral root production (Mallory et al., 2005). Another miRNA of Arabidopsis, miR164, has been shown to participate in regulating lateral root production by targeting the transcriptional activator NAC1 (Guo et al., 2005). Unlike NAC1, which is involved specifically in initiating lateral root formation (Xie et al., 2000), ARF10 and ARF16 may generally repress cell division. Thus, in the vascular bundle, the targeting of *ARF* transcripts by miR160 for degradation provides a condition that supports lateral root production.

Data obtained from IAA and NPA treatment experiments suggest that miR160 expression does not respond to auxin signals (Figures 5O and 5P; see Supplemental Figure 2 online). The miR160 production may be regulated cell autonomously; in lateral roots, for example, miR160 expression is activated in cells that have acquired vascular tissue status (Figure 4E). On the other hand, *ARF16* expression is auxin-inducible, and in roots its expression is linked to the auxin response maximum (Figure 5). These results indicate that auxin signals are involved in activating *ARF16* transcription. We propose that miR160 plays a role in connecting the developmental programs to the auxin signaling network by downregulating a subset of *ARF* genes. This is most evident in roots, in which auxin and miR160 regulate *ARF* expression independently, generating a spatial pattern for continuous root cap cell formation and lateral root production. In aerial organs, such as leaf, although we did not find a tissue-specific pattern, miR160 expression is low in young leaves and high in old leaves; in this way, miR160 gradually downregulates target *ARF* gene expression during leaf development.

The expression of *mARF16*, which is miR160-uncoupled, causes many abnormalities in plant development; such pleiotropic effects are often observed on plants harboring dominant mutations of the *AUX/IAA* genes, which encode repressors of the ARFs (Gray et al., 2001). The ubiquitin-mediated proteolysis of AUX/IAAs is probably the primary mechanism for modulating ARF activity and hence the auxin response. In addition, miR160 adds another modulator to the auxin signaling network: regulating a subset of *ARF* genes at the posttranscriptional level. Although the role of ARF10 and ARF16 in controlling root cap cell development is evident, the relation between the miR160-targeted ARFs and the auxin response is complex and intriguing. Based on the increased expression of early auxin response genes and the *DR5* reporter in *Pro$_{ARF16}$:mARF16* plants, ARF16 should act as a positive regulator of auxin signaling. However, phenotypes of the transgenic and double mutant plants, such as the reduced lateral root number and aerial organ size of *Pro$_{ARF16}$:mARF16* plants, suggest a negative role of ARF16 in the auxin response. It is well known that exogenous IAA at very low concentrations stimulates cell division and root growth, whereas at high concentrations it plays a negative role. Thus, a plausible explanation is that, by targeting a group of *ARF* genes, miR160 helps to control the basal expression of auxin response genes within the threshold level, which varies in different tissues and at different developmental stages. Another possibility is that ARF16 and related ARF proteins generally inhibit cell division and growth, and miR160, which itself is developmentally regulated, promotes cell division and growth by downregulating these *ARF* genes. Although the role of the miR160-target ARFs in relation to auxin signaling needs further investigation, there is little doubt that this miRNA-based regulation is essential for Arabidopsis development and growth.

## METHODS

### Plant Materials

Plants of *Arabidopsis thaliana* (Columbia [Col-0] ecotype) and tobacco (*Nicotiana benthamiana*) were grown under continuous-light conditions at 22°C. The GFP and GUS marker lines were used as described by Sabatini et al. (1999). All marker lines were delivered into *Pro$_{35S}$:MIR160c*, *Pro$_{ARF16}$:ARF16*, or *Pro$_{ARF16}$:mARF16* plants by crossing. *arf16-2* (SALK_021448) (Alonso et al., 2003), *pin1* (CS8065), *axr1-3* (CS3075), *mp$^{U55}$* (CS8147), and *tir1-1* (CS3798) mutants were obtained from the ABRC (Ohio State University, Columbus, OH). *arf10-2* (FLAG_442E12) (Samson et al., 2002) was ordered from the Institut National de la Recherche

Agronomique (Versailles, France). Before analysis, *arf10-2* (Wassilewskija ecotype) was outcrossed twice, and *arf16-2* (Col-0 ecotype) was backcrossed twice, to the Col-0 wild-type plants. For vertical plate growth, seeds were surface-sterilized for 10 min in 30% (v/v) bleach containing 0.01% Triton X-100, washed four times with sterile water, and synchronized at 4°C for 72 h. The seeds were sown on half-strength MS agar plates (Sigma-Aldrich, St. Louis, MO) with or without 5 μM NPA. The plates were vertically placed under continuous light at 22°C for the periods indicated in the figures. For auxin induction, 7-d-old vertically growing seedlings were placed in liquid half-strength MS medium supplemented with IAA at the concentrations indicated in the figures. The seedlings were harvested and stored at −70°C before analysis.

### Identification of T-DNA Insertion Mutants

PCR with left border primers (LB4 for *ARF10*, 5′-CGTGTGCCAGGTGCCCACGGAATAGT-3′; LBb1 for *ARF16*, 5′-GCGTGGACCGCTTGCTGCAACT-3′) and gene-specific primers (*ARF10*, 5′-TAGGATTCCGCAGCCATTTGA-3′ and 5′-CTCACGTTGTCGCCACCAATA-3′; *ARF16*, 5′-CCTGGCTCCCTGTAAACCCAC-3′ and 5′-CCTCGGCGTCACCTTCTTACA-3′) was used to identify T-DNA insertion mutants of *arf10-2* and *arf16-2*, respectively. The insertion sites were verified by sequencing of T-DNA left border flanking sequences. The T-DNA insertion site of the *arf10-2* mutant is 1856 bp, and that of *arf16-2* is 1112 bp, downstream of the translation start codon. The homozygous *arf10-2 arf16-2* double mutant was screened in the F2 generation, and F3 plants were used for phenotypic analyses.

### Vector Construction and Plant Transformation

Plasmids for miR160 overexpression were generated by cloning 1-kb intergenic genomic fragments of *MIR160a*, *-b*, or *-c* to the transgenic vector pKYLX71 (Schardl et al., 1987). The promoter regions (~2 kb) of *MIR160c*, *ARF10*, *ARF16*, and *ARF17* were amplified by PCR. The point mutations of *ARF10*, *ARF16*, and *ARF17* cDNAs were created by two-round PCR and confirmed by DNA sequencing. $Pro_{35S}$*:ARF16*, $Pro_{35S}$*:mARF16*, $Pro_{ARF16}$*:ARF16*, and $Pro_{ARF16}$*:mARF16* vectors were constructed by cloning the wild-type or mutated cDNAs into pCAMBIA1300 harboring either the *35S* or the *pARF16* promoter.

For GUS- or GFP-ARF16 fusion proteins, coding sequences of GUS or GFP, respectively, were fused in-frame to *ARF16* cDNA, and the resulting fusions were inserted into pCAMBIA1300 carrying the promoter of *ARF16*. Transgenic Arabidopsis plants were generated by the floral dip method (Clough and Bent, 1998) and screened on solid plates containing 50 μg/mL hygromycin (pCAMBIA1300) or kanamycin (pKYLX71). Six independent single-insertion transgenic lines were identified in the T3 generation based on antibiotic resistance and used subsequently for phenotypic analyses.

For transient analysis of the miR160 activity in tobacco, *Agrobacterium tumefaciens* cells harboring the constructs were injected into leaves of 3-week-old tobacco plants (Llave et al., 2002).

### Microscopy

Plant materials were fixed in a solution of 5% (v/v) acetic acid, 45% (v/v) ethanol, and 5% (v/v) formaldehyde at 4°C overnight and dehydrated in series with ethanol. For scanning electron microscopy, the samples were critical point dried in liquid carbon dioxide and coated with gold, followed by visualization with the JSM-6360LV scanning electron microscope (JEOL, Tokyo, Japan). For histological sections, samples were embedded in Epon812 resin, and transverse sections were made at 2 μm. Cell walls were stained by toluidine blue, and sections were examined microscopically (BX51; Olympus, Tokyo, Japan) and photographed.

Confocal images were obtained with a LSM510 laser scanning confocal microscope (Zeiss, Jena, Germany) with argon laser excitation at 488 nm and a 505- to 550-nm emission filter set for GFP fluorescence observation. The cell walls of root tips were visualized by staining with 10 μg/mL propidium iodide. The embryos were dissected and mounted on 5% glycerol without fixation.

### Phenotypic Analyses

The primary root length and lateral root number were scored from 9-d-old seedlings grown on a vertical plate. GUS and starch granule staining were performed as described (Willemsen et al., 1998). Samples were mounted on 50% glycerol and photographed using differential interference contrast optics. For gravitropic analysis, the 4-d-old vertically grown seedlings were rotated 90° clockwise. The root tip positions, before and 12 h after rotation, were recorded.

### RNA Analysis

Total RNAs were isolated from plant materials using Trizol reagent according to the manufacturer's manual (Invitrogen, Carlsbad, CA). The RNAs, 20 μg in each lane, were separated on a 1.0% denaturing gel and transferred to a Hybond-$N^+$ filter membrane (Amersham Pharmacia Biotech, Uppsala, Sweden). For small RNAs, 20 μg of RNA was dissolved on a Tris-borate-EDTA urea gel (15%) and electroblotted onto a Hybond-$N^+$ membrane. The membrane was UV cross-linked and hybridized with ExpressHyb solution (Clontech, Palo Alto, CA). miR160 probes were prepared by end-labeling antisense oligonucleotides using T4 polynucleotide kinase (New England Biolabs, Beverly, MA). For *ARF10*, *ARF16*, and *ARF17*, the probes were randomly labeled with $^{32}$P-dCTP using the 3′ cDNA fragments behind the miRNA recognition site as templates. RT-PCR was performed according to the protocols described by Xu et al. (2004) and Sorin et al. (2005). All PCR primer sequences are available upon request.

The Arabidopsis Genome Initiative locus numbers for *ARF10*, *ARF16*, and *ARF17* are At2g28350, At4g30080, and At1g77850, respectively.

## ACKNOWLEDGMENTS

We thank Ben Scheres for the *DR5-GUS* and *QC25* plants, John Celenza for the $Pro_{cyc1At}$*:CDB-GUS* plant, the ABRC for the *arf16-2* T-DNA insertion mutant and root tip GFP marker lines, and the Institut National de la Recherche Agronomique for the *arf10-2* T-DNA mutant. We are grateful to Meng-Min Hong, Zhi-Hong Xu, Hong-Quan Yang, and Xiao-Yan Gao for their suggestions and assistance. This research was supported by the National Science Foundation of China (Grant 30421001).

Received March 31, 2005; revised June 16, 2005; accepted June 17, 2005; published July 8, 2005.

## REFERENCES

**Adai, A., Johnson, C., Mlotshwa, S., Archer-Evans, S., Manocha, V., Vance, V., and Sundaresan, V.** (2005). Computational prediction of miRNAs in *Arabidopsis thaliana*. Genome Res. **15,** 78–91.

**Aida, M., Beis, D., Heidstra, R., Willemsen, V., Blilou, I., Galinha, C., Nussaume, L., Noh, Y.S., Amasino, R., and Scheres, B.** (2004). The *PLETHORA* genes mediate patterning of the Arabidopsis root stem cell niche. Cell **119,** 109–120.

**Alonso, J.M., et al.** (2003). Genome-wide insertional mutagenesis of *Arabidopsis thaliana*. Science **301,** 653–657.

**Bartel, D.P.** (2004). MicroRNAs: Genomics, biogenesis, mechanism, and function. Cell **116,** 281–297.

**Berleth, T., and Jürgens, G.** (1993). The role of the *MONOPTEROS* gene in organizing the basal body region of the embryo. Development **118,** 575–587.

**Birnbaum, K., Shasha, D.E., Wang, J.Y., Jung, J.W., Lambert, G.M., Galbraith, D.W., and Benfey, P.N.** (2003). A gene expression map of the Arabidopsis root. Science **302,** 1956–1960.

**Blilou, I., Frugier, F., Folmer, S., Serralbo, O., Willemsen, V., Wolkenfelt, H., Eloy, N.B., Ferreira, P., Weisbeek, P., and Scheres, B.** (2002). The Arabidopsis *HOBBIT* gene encodes a CDC27 homolog that links the plant cell cycle to progression of cell differentiation. Genes Dev. **16,** 2566–2575.

**Blilou, I., Xu, J., Wildwater, M., Willemsen, V., Paponov, I., Friml, J., Heidstra, R., Aida, M., Palme, K., and Scheres, B.** (2005). The PIN auxin efflux facilitator network controls growth and patterning in Arabidopsis roots. Nature **433,** 39–44.

**Bonnet, E., Wuyts, J., Rouzé, P., and Peer, Y.V.** (2004). Detection of 91 potential conserved plant microRNAs in *Arabidopsis thaliana* and *Oryza sativa* identifies important target genes. Proc. Natl. Acad. Sci. USA **101,** 11511–11516.

**Brand, U., Fletcher, J.C., Hobe, M., Meyerowitz, E.M., and Simon, R.** (2000). Dependence of stem cell fate in Arabidopsis on a feedback loop regulated by *CLV3* activity. Science **289,** 617–619.

**Clough, S.J., and Bent, A.F.** (1998). Floral dip: A simplified method for *Agrobacterium*-mediated transformation of *Arabidopsis thaliana*. Plant J. **16,** 735–743.

**Dharmasiri, N., and Estelle, M.** (2004). Auxin signaling and regulated protein degradation. Trends Plant Sci. **9,** 302–308.

**Di Laurenzio, L., Wysocka-Diller, J., Malamy, J.E., Pysh, L., Helariutta, Y., Freshour, G., Hahn, M.G., Feldmann, K.A., and Benfey, P.N.** (1996). The *SCARECROW* gene regulates an asymmetric cell division that is essential for generating the radial organization of the Arabidopsis root. Cell **86,** 423–433.

**Dolan, L., Janmaat, K., Willemsen, V., Linstead, P., Poethig, S., Roberts, K., and Scheres, B.** (1993). Cellular organisation of the *Arabidopsis thaliana* root. Development **119,** 71–84.

**Donnelly, P.M., Bonetta, D., Tsukaya, H., Dengler, R.E., and Dengler, N.G.** (1999). Cell cycling and cell enlargement in developing leaves of Arabidopsis. Dev. Biol. **215,** 407–419.

**Friml, J., Benková, E., Blilou, I., Wisniewska, J., Hamann, T., Ljung, K., Woody, S., Sandberg, G., Scheres, B., Jürgens, G., and Palme, K.** (2002). AtPIN4 mediates sink-driven auxin gradients and root patterning in Arabidopsis. Cell **108,** 661–673.

**Goda, H., Sawa, S., Asami, T., Fujioka, S., Shimada, Y., and Yoshida, S.** (2004). Comprehensive comparison of auxin-regulated and brassinosteroid-regulated genes in Arabidopsis. Plant Physiol. **134,** 1555–1573.

**Gray, W.M., Kepinski, S., Rouse, D., Leyser, O., and Estelle, M.** (2001). Auxin regulates $SCF^{TIR1}$-dependent degradation of AUX/IAA proteins. Nature **414,** 271–276.

**Guilfoyle, T.J., and Hagen, G.** (2001). Auxin response factors. J. Plant Growth Regul. **20,** 281–291.

**Guo, H.S., Xie, Q., Fei, J.F., and Chua, N.H.** (2005). MicroRNA directs mRNA cleavage of the transcription factor *NAC1* to downregulate auxin signals for Arabidopsis lateral root development. Plant Cell **17,** 1376–1386.

**Han, M.H., Goud, S., Song, L., and Fedoroff, N.** (2004). The Arabidopsis double-stranded RNA-binding protein HYL1 plays a role in microRNA-mediated gene regulation. Proc. Natl. Acad. Sci. USA **101,** 1093–1098.

**Hardtke, C.S., and Berleth, T.** (1998). The Arabidopsis gene *MONOPTEROS* encodes a transcription factor mediating embryo axis formation and vascular development. EMBO J. **17,** 1405–1411.

**Hardtke, C.S., Ckurshumova, W., Vidaurre, D.P., Singh, S.A., Stamatiou, G., Tiwari, S.B., Hagen, G., Guilfoyle, T.J., and Berleth, T.** (2004). Overlapping and non-redundant functions of the Arabidopsis auxin response factors *MONOPTEROS* and *NONPHOTOTROPIC HYPOCOTYL 4*. Development **131,** 1089–1100.

**Harper, R.M., Stowe-Evans, E.L., Luesse, D.R., Muto, H., Tatematsu, K., Watahiki, M.K., Yamamoto, K., and Liscum, E.** (2000). The *NPH4* locus encodes the auxin response factor *ARF7*, a conditional regulator of differential growth in aerial Arabidopsis tissue. Plant Cell **12,** 757–770.

**Helariutta, Y., Fukaki, H., Wysocka-Diller, J., Nakajima, K., Jung, J., Sena, G., Hauser, M.T., and Benfey, P.N.** (2000). The *SHORT-ROOT* gene controls radial patterning of the Arabidopsis root through radial signaling. Cell **101,** 555–567.

**Jones-Rhoades, M.W., and Bartel, D.P.** (2004). Computational identification of plant microRNAs and their targets, including a stress-induced miRNA. Mol. Cell **14,** 787–799.

**Lenhard, M., and Laux, T.** (2003). Stem cell homeostasis in the Arabidopsis shoot meristem is regulated by intercellular movement of CLAVATA3 and its sequestration by CLAVATA1. Development **130,** 3163–3173.

**Leyser, H.M., Pickett, F.B., Dharmasiri, S., and Estelle, M.** (1996). Mutations in the *AXR3* gene of Arabidopsis result in altered auxin response including ectopic expression from the *SAUR-AC1* promoter. Plant J. **10,** 403–413.

**Li, H., Johnson, P., Stepanova, A., Alonso, J.M., and Ecker, J.R.** (2004). Convergence of signaling pathways in the control of differential cell growth in Arabidopsis. Dev. Cell **7,** 193–204.

**Llave, C., Xie, Z., Kasschau, K.D., and Carrington, J.C.** (2002). Cleavage of *Scarecrow-like* mRNA targets directed by a class of Arabidopsis miRNA. Science **297,** 2053–2056.

**Lu, C., and Fedoroff, N.** (2000). A mutation in the Arabidopsis *HYL1* gene encoding a dsRNA binding protein affects responses to abscisic acid, auxin, and cytokinin. Plant Cell **12,** 2351–2366.

**Mallory, A.C., Bartel, D.P., and Bartel, B.** (2005). MicroRNA-directed regulation of Arabidopsis *AUXIN RESPONSE FACTOR17* is essential for proper development and modulates expression of early auxin response genes. Plant Cell **17,** 1360–1375.

**Nemhauser, J.L., Feldman, L.J., and Zambryski, P.C.** (2000). Auxin and *ETTIN* in Arabidopsis gynoecium morphogenesis. Development **127,** 3877–3888.

**Okushima, Y., et al.** (2005). Functional genomic analysis of the *AUXIN RESPONSE FACTOR* gene family members in *Arabidopsis thaliana*: Unique and overlapping functions of *ARF7* and *ARF19*. Plant Cell **17,** 444–463.

**Ouellet, F., Overvoorde, P.J., and Theologis, A.** (2001). IAA17/AXR3: Biochemical insight into an auxin mutant phenotype. Plant Cell **13,** 829–841.

**Reinhart, B.J., Weinstein, E.G., Rhoades, M.W., Bartel, B., and Bartel, D.P.** (2002). MicroRNAs in plants. Genes Dev. **16,** 1616–1626.

**Remington, D.L., Vision, T.J., Guilfoyle, T.J., and Reed, J.W.** (2004). Contrasting modes of diversification in the *Aux/IAA* and *ARF* gene families. Plant Physiol. **135,** 1738–1752.

**Rhoades, M.W., Reinhart, B.J., Lim, L.P., Burge, C.B., Bartel, B., and Bartel, D.P.** (2002). Prediction of plant microRNA targets. Cell **110,** 513–520.

**Rouse, D., Mackay, P., Stirnberg, P., Estelle, M., and Leyser, O.** (1998). Changes in auxin response from mutations in an *AUX/IAA* gene. Science **279,** 1371–1373.

**Sabatini, S., Beis, D., Wolkenfelt, H., Murfett, J., Guilfoyle, T., Malamy, J., Benfey, P., Leyser, O., Bechtold, N., Weisbeek, P.,**

**and Scheres, B.** (1999). An auxin-dependent distal organizer of pattern and polarity in the Arabidopsis root. Cell **99,** 463–472.

**Sabatini, S., Heidstra, R., Wildwater, M., and Scheres, B.** (2003). SCARECROW is involved in positioning the stem cell niche in the Arabidopsis root meristem. Genes Dev. **17,** 354–358.

**Sack, F.D.** (1997). Plastids and gravitropic sensing. Planta **203** (suppl.), S63–S68.

**Samson, F., Brunaud, V., Balzergue, S., Dubreucq, B., Lepiniec, L., Pelletier, G., Caboche, M., and Lecharny, A.** (2002). FLAGdb/FST: A database of mapped flanking insertion sites (FSTs) of *Arabidopsis thaliana* T-DNA transformants. Nucleic Acids Res. **30,** 94–97.

**Schardl, C.L., Byrd, A.D., Benzion, G., Altschuler, M.A., Hildebrand, D.F., and Hunt, A.G.** (1987). Design and construction of a versatile system for the expression of foreign genes in plants. Gene **61,** 1–11.

**Scheres, B., Benfey, P., and Dolan, L.** (2002). Root development. In The Arabidopsis Book, C.R. Somerville and E.M. Meyerowitz, eds (Rockville, MD: American Society of Plant Biologists), doi/10.1199/tab.0101, http://www.aspb.org/publications/arabidopsis/.

**Schoof, H., Lenhard, M., Haecker, A., Mayer, K.F., Jürgens, G., and Laux, T.** (2000). The stem cell population of Arabidopsis shoot meristems is maintained by a regulatory loop between the *CLAVATA* and *WUSCHEL* genes. Cell **100,** 635–644.

**Serino, G., and Deng, X.W.** (2003). The COP9 signalosome: Regulating plant development through the control of proteolysis. Annu. Rev. Plant Biol. **54,** 165–182.

**Sorin, C., Bussell, J.D., Camus, I., Ljung, K., Kowalczyk, M., Geiss, G., McKhann, H., Garcion, C., Vaucheret, H., Sandberg, G., and Bellini, C.** (2005). Auxin and light control of adventitious rooting in Arabidopsis require ARGONAUTE1. Plant Cell **17,** 1343–1359.

**Stowe-Evans, E.L., Harper, R.M., Motchoulski, A.V., and Liscum, E.** (1998). NPH4, a conditional modulator of auxin-dependent differential growth responses in Arabidopsis. Plant Physiol. **118,** 1265–1275.

**Sunkar, R., and Zhu, J.K.** (2004). Novel and stress-regulated microRNAs and other small RNAs from Arabidopsis. Plant Cell **16,** 2001–2019.

**Ulmasov, T., Murfett, J., Hagen, G., and Guilfoyle, T.J.** (1997). Aux/IAA proteins repress expression of reporter genes containing natural and highly active synthetic auxin response elements. Plant Cell **9,** 1963–1971.

**van den Berg, C., Willemsen, V., Hendriks, G., Weisbeek, P., and Scheres, B.** (1997). Short-range control of cell differentiation in the Arabidopsis root meristem. Nature **390,** 287–289.

**Vazquez, F., Gasciolli, V., Crété, P., and Vaucheret, H.** (2004). The nuclear dsRNA binding protein HYL1 is required for microRNA accumulation and plant development, but not post-transcriptional transgene silencing. Curr. Biol. **14,** 346–351.

**Weigel, D., and Jürgens, G.** (2002). Stem cells that make stems. Nature **415,** 751–754.

**Willemsen, V., Wolkenfelt, H., de Vrieze, G., Weisbeek, P., and Scheres, B.** (1998). The *HOBBIT* gene is required for formation of the root meristem in the Arabidopsis embryo. Development **125,** 521–531.

**Xie, Q., Frugis, G., Colgan, D., and Chua, N.H.** (2000). Arabidopsis NAC1 transduces auxin signal downstream of TIR1 to promote lateral root development. Genes Dev. **14,** 3024–3036.

**Xu, Y.H., Wang, J.W., Wang, S., Wang, J.Y., and Chen, X.Y.** (2004). Characterization of GaWRKY1, a cotton transcription factor that regulates the sesquiterpene synthase gene *(+)-delta-cadinene synthase-A*. Plant Physiol. **135,** 507–515.

**Zuker, M.** (2003). Mfold web server for nucleic acid folding and hybridization prediction. Nucleic Acids Res. **31,** 3406–3415.